Preparation, Structure and Reactivity of the Binuclear Di-μ-oxo-bis[(ethylenediamine-*N,N,N',N'*-tetraacetato)-rhenate(IV)] Complex†

Shinji Ikari,[a] Tasuku Ito,*[,a] William McFarlane,[c] Mohamed Nasreldin,[c] Bee-Lean Ooi,[c] Yoichi Sasaki*[,b] and A. Geoffrey Sykes*[,c]

[a] *Department of Chemistry, Faculty of Science, Tohoku University, Sendai 980, Japan*
[b] *Department of Chemistry, Faculty of Science, Hokkaido University, Sapporo 060, Japan*
[c] *Department of Chemistry, University of Newcastle, Newcastle upon Tyne NE1 7RU, UK*

The dark brown dirhenium(IV) complex $Ba_2[Re_2(\mu\text{-}O)_2(edta)_2]\cdot 4.5H_2O$ (H_4edta = ethylenediamine-*N,N,N',N'*-tetraacetic acid), peak at 450 nm (ε = 7880 M^{-1} cm^{-1} per dimer), has been prepared. From X-ray crystallography, the compound crystallizes in a monoclinic space group *C*2/*c* with *a* = 15.867(3), *b* = 12.914(2), *c* = 9.686(2) Å, β = 123.40(1)° and *Z* = 4. The structure is centrosymmetric, with the Re atoms having distorted octahedral co-ordination, and each tetradentate $edta^{4-}$ ligand having two unco-ordinated $-CH_2CO_2^-$ groups. The Re_2O_2 ring is planar and the short Re–Re distance of 2.362(2) Å is consistent with multiple metal–metal bonding. The structure is that of the *meso* ΔΛ form. The ^1H and ^{13}C NMR spectra of the uncrystallised sodium salt in aqueous solution (pH 7.5) provide evidence for both *meso* ΔΛ and racemic ΔΔ or ΛΛ forms. The UV–VIS and CD spectra of the (*R*)-pdta analogue, where $pdta^{4-}$ is propylenediamine-*N,N,N',N'*-tetraacetate, are also reported. The edta complex exhibits irreversible electrochemical behaviour with an oxidation wave at +1.23 V *vs.* the normal hydrogen electrode at $[H^+]$ = 0.10 M. Kinetic studies on the oxidation of the Re^{IV}_2 complex to Re^{VII} with the one-equivalent reagent *cis*-$[VO_2(H_2O)_4]^+$ in 1 M H^+ indicate a rate-determining first stage with no evidence for stable intermediate states. Effects of the product $[VO(H_2O)_5]^{2+}$ and H^+ on the kinetics, and an unexpected difference in reactivity of isomeric forms of the Re^{IV}_2 complex are reported.

The aqueous solution chemistry of the Group 7 elements technetium and rhenium is a somewhat neglected area which merits increased attention.[1,2] Much more work is required before the behaviour and properties of these elements are as well understood as for example those of Group 6 molybdenum and tungsten.[3] Whereas ethylenediaminetetraacetate (edta) complexes of molybdenum in the oxidation states III to VI,[4–11] and of tungsten in the V state,[12] have been reported, the only well documented Group 7 edta complex is that of the technetium(IV) dimer $[Tc_2(\mu\text{-}O)_2(H_2edta)_2]$.[13] As a platform to studies on rhenium chemistry we thought it important to develop further the chemistry with edta as a ligand. Some earlier studies on the Re^{IV}–edta complex[14] led to speculation concerning the structure, but with the information here reported the suggestions then made are no longer valid. The complex is fully characterised by a crystal structure determination, and studies include NMR detection of two isomers present in solution, IR on the solid, UV–VIS spectrophotometry, CD spectra of the related propylenediamine-tetraacetate (pdta) complex, as well as relevant electrochemical studies. We also describe the kinetics of the oxidation with V^V present as *cis*-$[VO_2(H_2O)_4]^+$ in aqueous acidic solutions, the initial aim of which was to identify edta complexes in other oxidation states. However a single rate-determining step only is observed in these studies and the final product is Re^{VII}.[15] The interplay of $[H^+]$ and $[V^{IV}]$ (product) dependencies indicates an important role of the unco-ordinated carboxylate ligands. Examples of oxo-, sulfido- and chloro-bridged dirhenium(IV) complexes have been reported previously, and diamagnetic Re≡Re triple bonds have been identified.[2,16,17]

‡ *Supplementary data available:* see Instructions for Authors, *J. Chem. Soc., Dalton Trans.*, 1993, Issue 1, pp. xxiii–xxviii.
Non-S.I. unit employed: M = mol dm^{-3}.

Experimental

Preparation of Sodium Di-μ-oxo-bis[{ethylenediamine-N,N,N',N'-tetraacetato)rhenate(IV)}] Octahydrate, $Na_4[Re_2(\mu\text{-}O)_2(edta)_2]\cdot 8H_2O$. Two procedures were used. In the first $Cs_2[ReOCl_5]$ (0.5 g, 0.8 mmol)[18] was added to a solution of sodium ethylenediamine-*N,N,N',N'*-tetraacetate tetrahydrate (0.38 g, 0.8 mmol) and sodium acetate (0.10 g, 1.2 mmol) in acetic acid (40 cm^3) and water (2 cm^3). Zinc dust (0.10 g, 1.5 mmol) was added, and the solution refluxed for 1 h. The remaining zinc dust was filtered off, and the filtrate evaporated to remove acetic acid. A brown powder was obtained by adding ethanol to the concentrate and filtering. Recrystallisation was from the minimum of water to which $NaClO_4$ (1g) had been added. On addition of ethanol a fine brown crystalline material was obtained. This was washed with ethanol and dried *in vacuo*; yield 0.34 g (70%) (Found: C, 19.70: H, 3.30: N, 4.60. Calc. for $C_{20}H_{40}N_4Na_4O_{26}Re_2$: C, 19.75; H, 3.30; N, 4.60%). IR (KBr disc): ν(Re–μ-O) 712 cm^{-1}. UV–VIS (aqueous solution): λ/nm (ε/M^{-1} cm^{-1}) 450 (7880), 582 (sh) (588), 608(sh) (267) and 751 (260).

In the second procedure $K_2[ReCl_6]$ (1 g, 2.1 mmol)[19] was added to 0.10 M acetate buffer at pH 4 containing disodium dihydrogenethylenediamine-*N,N,N',N'*-tetraacetate dihydrate (0.8 g). The solution was kept at 60 °C for 5 min with stirring. After 1 d a black precipitate was filtered off. The filtrate was diluted with water and loaded onto a QAE Sephadex A25 ion-exchange column in the Cl^- form. The column was washed with water, the brown band eluted with 2 M aqueous $NaClO_4$, and after concentrating the $NaClO_4$ filtered off. After leaving at 4 °C a brown powder was obtained. This was crystallised from water with the addition of ethanol, washed with ethanol and dried *in vacuo:* yield 0.64 g (50%). For NMR measurements a solution of $[Re_2(\mu\text{-}O)_2(edta)_2]^{4-}$ in ≈0.25 M NaCl from the QAE Sephadex

column was left to stand in a desiccator containing ethanol. Slow vaporisation/condensation of the ethanol into the solution of complex gave a brown powder. The solid was filtered off, washed with alcohol and diethyl ether and left to dry. For kinetic studies solutions eluted from a second QAE Sephadex column were used directly. At pH 5 solutions can be stored for weeks at 4 °C. No change in UV–VIS absorbance was observed for solutions in water kept under air for 2 d. In 0.01M acid [HCl, $HClO_4$ or toluene-*p*-sulfonic acid (Hpts)] at 25 °C the changes in absorbance observed were < 3% after 20 h.

Preparation of Sodium Di-μ-oxo-bis{[(R)-propylenediamine-N,N,N′,N′-tetraacetato]rhenate(IV)} Heptahydrate, $Na_4[Re_2(\mu\text{-}O)_2\{(R)\text{-pdta}\}_2]\cdot 7H_2O$.—The complex $Cs_2[ReOCl_5]$ (0.5 g, 0.8 mmol)[18] was added to a solution of (*R*)-propylenediamine-*N*,*N*,*N*′,*N*′-tetraacetic acid (0.25 g, 0.8 mmol)[20] and sodium acetate (0.1 g, 1.2 mmol) in an acetic acid (40 cm^3)–water (2 cm^3) mixture. After addition of zinc dust (0.1 g, 1.5 mmol) the solution was refluxed for 5 h and the remaining zinc dust filtered off. The filtrate was evaporated to remove acetic acid and passed through a Sephadex G-15 column. The eluate was concentrated after addition of $NaClO_4$ (0.5 g). A brown powder was filtered off, recrystallised from aqueous solution by adding ethanol, and finally washed with ethanol and dried *in vacuo*; yield 0.36 g (75%) (Found: C, 21.55; H, 3.35; N, 4.10. Calc. for $C_{22}H_{42}N_4Na_4O_{25}Re_2$: C, 21.55; H, 3.45; N, 4.55%. IR(KBr disc): ν(Re–μ-O) 712 cm^{-1}. UV–VIS (aqueous solution): λ/nm (ε/M^{-1} cm^{-1}) 453 (6280), 535(sh) (438), 600(sh) (195) and 756 (217). CD (aqueous solution): λ/nm (Δε/M^{-1} cm^{-1}), 230 (+5.4), 254 (−4.8), 378 (+12.3), 449 (−24.1), 546 (+0.37), and 612 (−0.70). The ^1H NMR spectrum indicated a mixture of two geometrical isomers. Attempts to separate the two using anion-exchange chromatography were unsuccessful.

Other Reagents.—Perchloric acid (70%) and disodium dihydrogenethylenediamine-*N*,*N*,*N*′,*N*′-tetraacetic acid were BDH AnalaR grade. Lithium perchlorate (Aldrich) was recrystallised twice from water. Solutions of the yellow *cis*-tetraaquadioxovanadium(V) ion, $[VO_2(H_2O)_4]^+$, in 2.0 M $HClO_4$ were prepared by dissolving a known amount of ammonium vanadate, NH_4VO_3 (BDH, AnalaR), in hot water followed by addition of an equal volume of 4.0 M $HClO_4$ with stirring. The concentration of V^V was determined by titration against a freshly prepared standard solution of ammonium iron(II) sulfate, using ferroin as indicator. Solutions of pentaaquaoxovanadium(IV), $[VO(H_2O)_5]^{2+}$, were obtained by loading a saturated solution of hydrated vanadium(IV) sulfate $VO(SO_4)$ (BDH, Reagent Grade) in 0.1M $HClO_4$ onto a Dowex 50W-X2 cation-exchange column, washing with distilled water to remove the sulfate, and eluting the vanadium(IV) with 1.0M $HClO_4$. Solutions were standardised spectrophotometrically at the 760 nm peak (ε = 17.2 M^{-1} cm^{-1}). Solutions of Ca^{2+} and La^{3+} were prepared by dissolving $CaCl_2$ (BDH, AnalaR) or $La(pts)_3$ in water. The latter was prepared by dissolving La_2O_3 (Aldrich, 99.99%) in toluene-*p*-sulfonic acid (Aldrich) and recrystallising twice from water. Solutions of TiO^{2+} were prepared by slow addition of $TiCl_4$ (Aldrich, 99.9%) from a syringe into 1.0 M $HClO_4$.

Equipment and Procedures.—All UV–VIS spectra were recorded on Perkin Elmer Lambda 9 and Hitachi 340 spectrophotometers, CD spectra on a JASCO J-40 automatic recording spectropolarimeter and infrared spectra on a JASCO IR-810 spectrophotometer in KBr pellets at room temperature. Proton and ^{13}C NMR spectra were measured on a JEOL GSX-270 FT spectrometer at 270 and 67.9 MHz, and at 500.14 and 125.77 MHz on a Bruker AMX500 spectrometer. Chemical shifts were recorded with an internal reference as indicated. The electrochemical measurement was carried out in aqueous solution by using a Yanaco P-1100 polarographic analyzer with a glassy carbon working electrode at 24 ± 2 °C. Reduction potentials quoted are *vs.* the normal hydrogen electode (NHE).

Crystal Structure Determination.—X-Ray structural determination of the edta complex was carried out with the barium salt. Crystals of $Ba_2[Re_2(\mu\text{-}O)_2(edta)_2]\cdot 4.5H_2O$ were obtained by keeping an aqueous solution of the sodium salt in 0.5 M barium chloride for 1 week under slow diffusion of ethanol. A single crystal (0.15 × 0.08 × 0.05 mm) was glued with epoxy resin to a glass fibre and mounted on a Rigaku AFC-5R four-circle diffractometer equipped with a rotating anode (50 kV, 120 mA) and graphite-monochromated Mo-Kα radiation (λ = 0.710 69 Å). The unit-cell parameters were obtained by a least-squares refinement of the angular settings of 40 reflections (25 < 2θ < 30°). Crystallographic data and data collection parameters are summarised in Table 1. Intensity data were corrected for Lorentz and polarisation factors. Absorption corrections were made according to the method used for a polyhedral model.[21] Atomic scattering factors were taken from ref. 22.

The structure was solved by the heavy-atom method and refined by the block-diagonal least-squares method. The function used in the least-squares minimisation was $\Sigma w[|F_o| - |F_c|]^2$, where $w = 1/\sigma^2(|F_o|)$. The structure was successfully solved assuming a space group *C*2/*c* from the three possibilities (*C*2, *Cm* and *C*2/*c*) determined by the systematic extinction method (*hkl*: *h* + *k* = 2*n*. *h*01: *h* = 2*n* 0*k*0: *k* = 2*n*). Anisotropic thermal parameters were applied to all non-hydrogen atoms. All the water molecules (4.5 per anion) were successfully located. The final refinement gave *R* = 0.029. Hydrogen atoms were not included in the analysis.

All calculations were performed with the Universal Crystallographic Computer Program System UNICS III[23] on a ACOS-2000 computer at the Computer Centre of Tohoku University. Atomic positional parameters are given in Table 2.

Additional material available from the Cambridge Crystallographic Data Centre comprises H-atom coordinates, thermal parameters and remaining bond distances and angles.

Redox Properties.—Cyclic voltammograms of the edta complex in aqueous phosphate buffer solutions at pH 7.5 gave only one irreversible oxidation wave at +1.29 V in the range −1.26 to +1.75 V *vs.* NHE, and no reduction wave. At $[H^+]$ = 0.10 M, *I* = 1.00 M ($NaClO_4$) at a glassy carbon-disc (working) and platinum electrodes an irreversible peak was observed at 1.23V. Reversible one-electron reduction steps have been observed previously for ditechnetium(IV) complexes, *e.g.* the dimer $[Tc_2(\mu\text{-}O)_2(tcta)_2]^{2-}$ (tcta = 1,4,7-triazacyclononane-*N*,*N*′,*N*″-triacetate) at 0.41V *vs.* NHE.[24] The structure of the $Tc^{III}Tc^{IV}$ product has been reported.[24] Also the H_2edta^{2-} and nta^{3-} (nta = nitrilotriacetate) complexes of $Tc^{IV}{}_2$ are easily reduced to the $Tc^{III}Tc^{IV}$ state by electrochemical means,[24] and chemically with hydrazine.[25] On the other hand di-μ-oxo-dirhenium(IV) complexes do not appear to be as readily reduced,[26] and Tc and Re conform to the general rule that the reduction of third-row as opposed to second-row transition metals is more difficult to bring about.

Kinetic Studies.—The stoichiometry of the vanadium(V) oxidation was determined by addition of 0.1 cm^3 aliquots of $[VO_2(H_2O)_4]^+$ (5 mM) to a solution of $[Re_2O_2(edta)_2]^{4-}$ (1.5 cm^3, 0.28 mM) in an optical cell. The decrease in absorbance at 450 nm (ε = 7880 M^{-1} cm^{-1} per rhenium dimer) was monitored, and an uptake of 5.89 ± 0.2 mol of V^V per mol of dimer (three determinations) was indicated. The reaction can therefore be written as in equation (1) where the rhenium(VII)

$$Re^{IV}{}_2 + 6V^V \rightarrow 2Re^{VII} + 6V^{IV} \quad (1)$$

product is most likely present as the perrhenate ion $[ReO_4]^-$. From a sample of $[NH_4][ReO_4]$ (Johnson Matthey) the latter

Table 1 Crystallographic data for $Ba_2[Re_2(\mu\text{-}O)_2(edta)_2]\cdot 4.5H_2O$

Formula	$C_{20}H_{33}Ba_2N_4O_{22.5}Re_2$
M	1308.55
Crystal symmetry	Monoclinic
Space group	$C2/c$
a/Å	15.867(3)
b/Å	12.914(2)
c/Å	9.686(2)
β/°	123.40(1)
U/Å^3	1659.9(5)
Z	4
μ	102.2 cm^{-1}
D_c/g cm^{-3}	2.59
D_m[a]/g cm^{-3}	2.63
T/°C	22
No. of unique reflections	3814
No. of observed reflections [($\|F_o\| > 3\sigma(F_o)$]	1924
No. of variables	146
$R(F_o)$[b]	0.0289[b]
$R'(F_o^2)$[c]	0.0297

[a] In $CHCl_3$–$CHBr_3$. [b] $R = \Sigma[|F_o| - |F_c|]/\Sigma|F_o|$. [c] $R' = [\Sigma w(|F_o| - |F_c|)^2/\Sigma|F_o|^2]^{\frac{1}{2}}$.

Table 2 Positional parameters ($\times 10^5$ for Re and Ba, $\times 10^4$ for other atoms) for $Ba_2[Re_2(\mu\text{-}O)_2(edta)_2]\cdot 4.5H_2O$

Atom	x	y	z
Re	0	9 129(3)	0
Ba	14 452(4)	50 000	67 723(6)
O(1)	−183(5)	0	−1 738(7)
O(2)	1 498(3)	1 074(4)	965(5)
O(3)	2 564(4)	1 224(5)	186(7)
O(4)	−208(4)	3 844(4)	−3 656(6)
O(5)	−1 513(5)	2 984(5)	−5 782(7)
N	51(4)	2 186(4)	−1 456(7)
C(1)	1 729(5)	1 370(5)	−70(8)
C(2)	906(5)	1 905(6)	−1 633(8)
C(3)	−847(6)	3 118(6)	−4 270(9)
C(4)	−901(5)	2 314(6)	−3 159(8)
C(5)	308(6)	3 140(5)	−387(8)
Ow(1)	−2 584(9)	5 000	−5 397(14)
Ow(2)	−2 379(11)	1 113(13)	−7 004(16)
Ow(3)	0	0	−5 000

is colourless with a UV band at 225 nm (ε = 3400 M^{-1} cm^{-1}), which is difficult to identify spectrophotometrically in the presence of V^V, V^{IV} and edta.

The kinetics of the vanadium(v) oxidation of $[Re_2O_2(edta)_2]^{4-}$ was studied under first-order conditions with the oxidant in >30-fold excess and under N_2. The decay of $[Re_2O_2(edta)_2]^{4-}$ was monitored at 450 nm. Biphasic kinetics were observed. The linear portion (second phase) of plots of absorbance (A) changes $\ln(A_t - A_\infty)$ against time gave first-order rate constants (k_{2obs}) for the second phase. Rate constants for the first phase (k_{1obs}) were obtained from the slope of a plot of $\ln[xe^{-k_{2obs}t} - (A_t - A_\infty)]$ against time, where x is the intercept at $t = 0$.

Results and Discussion

Crystal Structure.—The ORTEP[27] drawing of the anion in $Ba_2[Re_2(\mu\text{-}O)_2(edta)_2]\cdot 4.5H_2O$ is shown in Fig. 1. An asymmetric unit of the cell contains a quarter of this centrosymmetric complex ion. A two-fold axis passes through two Re atoms and there is a mirror plane containing two bridging oxo ligands perpendicular to the Re–Re axis. Important bond lengths and angles are summarised in Table 3. The two rhenium ions and the bridging oxo ligands form a planar Re_2O_2 unit. Each metal ion has distorted-octahedral co-ordination geometry involving a tetradentate edta with two

Table 3 Interatomic distances (Å) and angles (°) for $[Re_2(\mu\text{-}O)_2(edta)_2]^{4-}$

Re–Re′	2.3621(8)	Re–O(1)	1.943(6)
Re–O(2)	2.025(5)	Re–N	2.198(6)
O(2)–C(1)	1.30(1)	O(4)–C(3)	1.263(9)
O(3)–C(1)	1.22(1)	O(5)–C(3)	1.260(8)
N–C(2)	1.50(1)	N–C(4)	1.511(7)
C(1)–C(2)	1.516(8)	C(3)–C(4)	1.53(7)
N–C(5)	1.516(9)	C(5)–C(5′)	1.52(2)
Re′–Re–O(1)	52.6(1)	Re′–Re–O(2)	95.9(1)
Re′–Re–N	138.5(2)	O(1)–Re–O(2)	94.8(3)
O(1)–Re–N	166.1(2)	O(2)–Re–N	76.8(2)
O(1)–Re–O(1′)	105.1(2)	Re–O(1)–Re′	74.9(3)
Re–O(2)–C(1)	115.4(3)	N–Re–N′	83.0(2)
Re–N–C(2)	104.2(4)	Re–N–C(4)	114.6(5)
C(2)–N–C(5)	110.9(6)	C(4)–N–C(5)	112.8(5)
O(2)–C(1)–O(3)	122.1(6)	O(4)–C(3)–O(5)	126.2(8)
O(2)–C(1)–C(2)	117.0(7)	O(4)–C(3)–C(4)	120.9(6)
O(3)–C(1)–C(2)	121.0(8)	O(5)–C(3)–C(4)	112.8(7)
N–C(2)–C(1)	109.3(7)	N–C(4)–C(3)	115.7(6)
Re–N–C(5)	105.2(5)	N–C(5)–C(5′)	109.5(6)

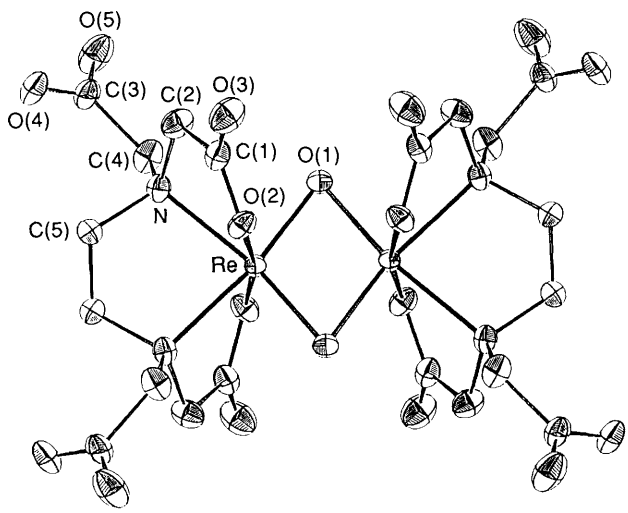

Fig. 1 Structure of the $[Re_2(\mu\text{-}O)_2(edta)_2]^{4-}$ ion and its atomic numbering scheme. The thermal ellipsoids are drawn at 50% probability

nitrogens co-ordinated *trans* to the oxo bridges. Two carboxylate arms co-ordinate in the *trans* position on each rhenium, and the two remaining carboxylate $-CH_2CO_2^-$ groups of the edta are associated with barium ions. The two N–O chelate rings to each rhenium make the rhenium co-ordination spheres optically active. However, the dimer structure observed is not optically active since it has the *meso* ($\Delta\Lambda$) configuration as expected for a centrosymmetric ion. The structure of the $Re^{IV}{}_2$–edta complex is very similar to that of $Tc^{IV}{}_2$–edta except that there is protonation of the two free carboxylate arms in the latter to give $[Tc_2(\mu\text{-}O)_2(H_2edta)_2]$.[13] The Re–Re distance of 2.362 Å is slightly longer than the corresponding Tc–Tc distance (2.331 Å), and is virtually identical to that in two other $Re_2(\mu\text{-}O)_2$ complexes.[2] It is however shorter than observed for $Re^{IV}{}_2(\mu\text{-}O)_2$ units in the oxides $Nd_4Re_2O_{11}$ (2.421 Å)[28] and $La_6Re_4O_{18}$ (2.456 Å).[29] Comparisons with $[Re^{IV}{}_2(\mu\text{-}O)(\mu\text{-}Cl)(\mu\text{-}EtCO_2)Cl_4(PPh_3)_2]$ (2.522 Å) and $[Re^{IV}{}_2(\mu\text{-}S)_2(S_2CNBu_2)_4]$ (2.546 Å) are also of interest.[16,17] The short Re–Re distance in the present case is consistent with a metal–metal multiple bond as discussed previously for $Re^{IV}{}_2(\mu\text{-}O)_2$ and $Tc^{IV}{}_2(\mu\text{-}O)_2$ complexes.[2,13,30]

The present structure is quite different from that of the isoelectronic molybdenum(III)–edta dimer $[Mo_2(\mu\text{-}OH)_2(\mu\text{-}MeCO_2)(\mu\text{-edta-}N,N')]^-$, which has an edta-$N,N'$-bridge with two carboxylate groups co-ordinated to each Mo.[5] It is unlikely that the different bridging groups and/or oxidation state causes

the different co-ordination mode of the edta, since the molybednum(v) dimer with a di-μ-oxo bridge has the same edta-*N*,*N*′-bridged structure.[7] The different synthetic routes may be responsible. Thus the edta bridging mode will be favoured in the case of the $Mo^{V}_2O_2(\mu\text{-}O)_2$ complex since only three co-ordination sites are available on each molybdenum(v). Also the Mo^{III}–edta dimer is prepared by reduction of the molybdenum(v) dimer in acetate buffer solution.[31,32]

Proton and ^{13}C *NMR Spectra.*—The ^1H NMR spectrum of unrecrystallised $[Re_2(\mu\text{-}O)_2(edta)_2]^{4-}$ solid made up in D_2O is shown in Fig. 2. It clearly indicates the presence of two isomers in about 2:1 amounts. These give similar, but not identical, spectra that are consistent with the presence of *meso* (ΔΛ) and racemic (ΔΔ or ΛΛ) configurations, although it is not possible to say which corresponds to the major component. The proportion of the minor isomer increases as the solution ages over a period of 2 weeks.

It is important to recognise that all of the three types of CH_2 group in each of these configurations (note that ΔΔ will give identical spectra to those of ΛΛ) have hydrogens that are diastereotopic, and in particular that even when there is unrestricted rotation about the C–N bond this will still apply to the unco-ordinated acetate group owing to its proximity to the chiral nitrogen atom. Thus both types of acetate should give AB patterns, and these are clearly observed for the major isomer at δ 4.40 and 5.56 with J = 17.3 Hz and at δ 5.15 and 5.53 with J = 17.5 Hz, and for the minor isomer at δ 4.32 and 5.61 with J = 17.0 Hz and at δ 5.22 and 5.52 with J = 17.6 Hz. On the basis of their smaller internal chemical shift differences the latter pair in each case is tentatively assigned to the free acetate. The ethylene hydrogens of each isomer form an AA′BB′ spin system with expected geminal couplings of *ca.* −14 Hz, and vicinal ones of 3–8 Hz, which give characteristic patterns at δ 4.34 and 4.47. This interpretation was fully confirmed by a two-dimensional double-quantum-filtered correlation spectroscopy (COSY) experiment. It should be noted that for these species the chemical shifts show marked temperature dependences, and consequently the appearance of the spectra is affected by the sample conditions.

There are no indications of exchange of free and co-ordinated acetates within the time-scale of the NMR measurement. Signals for the co-ordinated ligand appear at significantly higher frequency than those of the dimeric molybdenum and tungsten complexes. In the case of $[W_2O_4(edta)]^{2-}$ for example the protons of the ethylene and acetate arms give signals at δ 2.74 and 3.62 respectively.[12] This may be due to the stronger deshielding effect resulting from the higher degree of metal–metal bonding in the rhenium complex.

The (*R*)-pdta complex shows a fairly complicated ^1H NMR spectrum as expected from the non-equivalence of the hydrogens of the ligand. It should be noted that two sets of methyl doublet are observed in 7:1 integrated intensity ratio in the region δ 1.54–1.62 (neither of which is assigned to the free ligand). Other hydrogens are observed in the region δ 4.0–5.5 with expected integrated intensity ratio to the methyl signal. The pattern of methyl signals is interpreted by assuming the existence of the two geometrical isomers.

It is known that a methyl group attached to a diamine chelate ring prefers an equatorial orientation.[33] This would make the conformation of the (*R*)-propylenediamine chelate ring λ and accordingly restricts the configuration around the metal ion to Δ.[33] The complex is therefore optically active with respect to the chelate-ring arrangement and should have a ΔΔ configuration. Fig. 3 shows the two possible geometrical isomers of the (*R*)-pdta complex, both with a ΔΔ configuration. In each isomer two methyl groups are chemically equivalent. The two methyl doublets observed in the ^1H NMR spectra would indicate the existence of the two geometrical isomers in 7:1 ratio. It is not possible to assign the doublets to individual isomers. As indicated in the Experimental section, attempts to separate the complex into the different isomers by anion-exchange chromatography were unsuccessful.

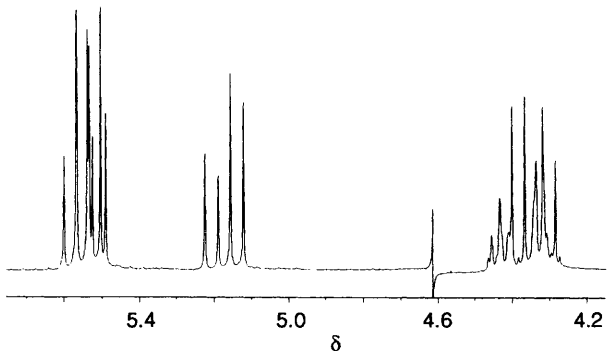

Fig. 2 The 500.14 MHz ^1H NMR spectrum of freshly precipitated $[Re_2(\mu\text{-}O)_2(edta)_2]^{4-}$ in D_2O at 75 °C. Shifts are in ppm relative to internal dioxane at δ 3.74

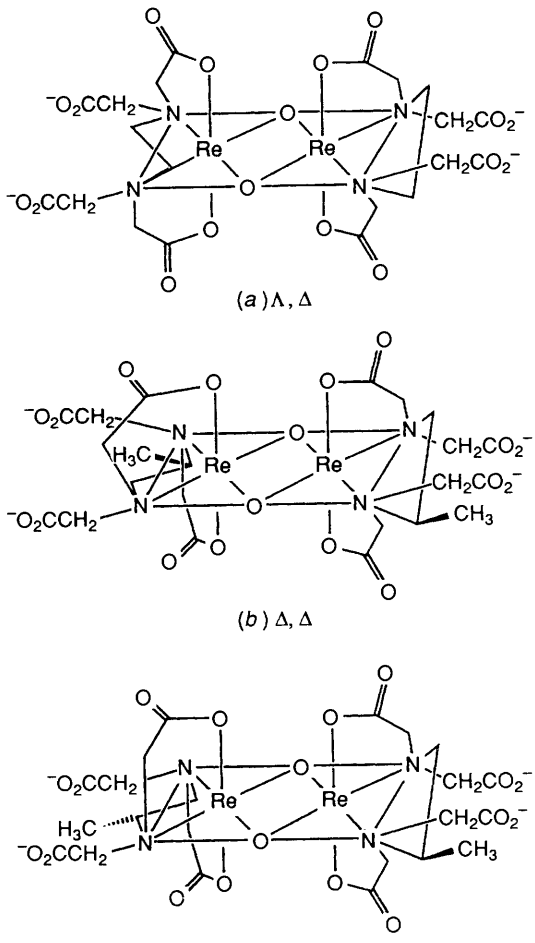

Fig. 3 Structures of (*a*) $[Re_2(\mu\text{-}O)_2(edta)_2]^{4-}$, and (*b*) and (*c*) two possible geometric isomers of $[Re_2(\mu\text{-}O)_2(pdta)_2]^{4-}$

The ^{13}C NMR spectrum of the crude edta complex in D_2O also confirmed the presence of two isomers. For the major isomer the methylene carbons of the acetates occur at δ 67.0 and 68.4, the former being appreciably broadened, the carbonyls at δ 176.9 and 183.1 and the backbone ethylene resonance at δ 59.2. For the minor isomer the corresponding resonances are δ 68.0 (br) and 68.3, 177.0 and 184.2, and 59.5.

Electronic and Circular Dichroism Spectra.—Fig. 4 shows the UV–VIS and circular dichroism (CD) spectra of $[Re_2(\mu\text{-}$

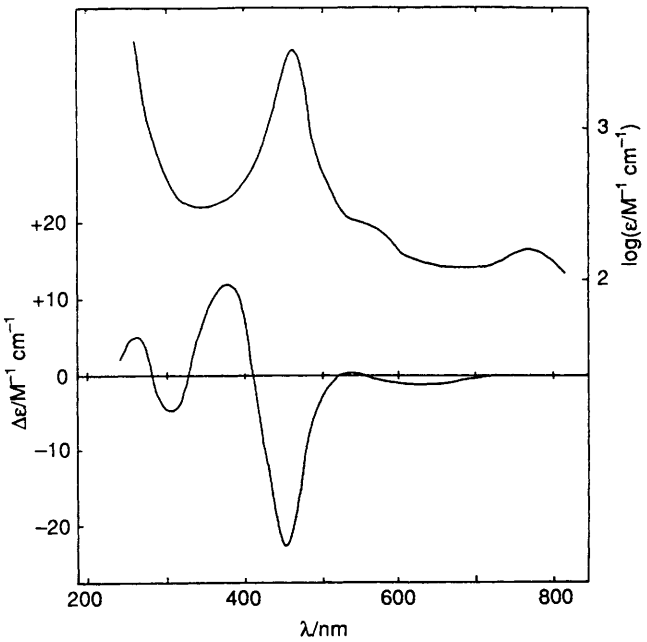

Fig. 4 Electronic (upper) and circular dichroism (lower) spectra of $Na_4[Re_2(\mu\text{-}O)_2\{(R)\text{-pdta}\}_2]\cdot 8H_2O$ in water at room temperature

Table 4 First-order rate constants (25 °C) for the oxidation of $[Re_2O_2(edta)_2]^{4-}$ with V^V, $[H^+] = 0.10$ M, $I = 1.00$ M ($LiClO_4$)

$10^3[Re^{IV}{}_2]$/M	$10^3[V^V]$/M	$10^3k_{1obs}/s^{-1}$	$10^3k_{2obs}/s^{-1}$
0.06	8.33	3.07	2.72[a]
	6.67	2.64	2.17[a]
	5.00	1.93	1.59[a]
		1.88	1.61
	4.50	1.78	1.50
	4.00	1.62	1.36
0.05	3.73	1.53	1.22[b]
	3.33	1.43	1.16
	3.00	1.29	1.03
	2.83	1.32	0.93[c]
	2.67	1.19	0.88[d]
	1.50	1.18	0.88
		1.13	0.85[e]
0.04	2.00	1.01	0.63
		1.03	0.73[f]
		1.02	0.71[e]
0.03	1.50	0.79	0.53
		0.80	0.51[e]
	1.00	0.62	0.38

[a] $[H^+] = 0.50$ M. [b] $[Cl^-] = 0.15$ M. [c] $[La^{3+}] = 4.80$ mM. [d] $[Ca^{2+}] = 4.77$ mM. [e] $[H^+] = 0.050$ M. [f] $[TiO^{2+}] = 4.80$ mM.

$O)_2\{(R)\text{-pdta}\}_2]^{4-}$. The edta analogue shows a very similar absorption spectrum. The UV–VIS spectrum is characterised by a strong band at 453 nm ($\varepsilon = 6280$ M^{-1} cm^{-1} per dimer) with smaller bands and shoulders in the visible region. The peak positions are similar to those of $[Re_2(\mu\text{-}O)_2X_2L]^{2+}$ (L = 1,4,7-triazacyclononane; X = Cl, Br or I) at 461, 477 and 497 nm respectively.[2b] The shift in absorbance bands of the edta complex to shorter wavelengths is consistent with the trend observed for the above halide complexes. The patterns observed are similar to those of the ditechnetium(IV) aminopolycarboxylate complexes,[13,24,34] *e.g.* 495 nm for the strong band of the isostructural $[Tc_2(\mu\text{-}O)_2(H_2edta)_2]$.[13] There are also similarities to the spectra of isoelectronic di-μ-hydroxo-dimolybdenum(III) and -ditungsten(III) complexes,[32,35,36] as indicated previously.[2] The strong absorption band for $[Mo_2(\mu\text{-}OH)_2(\mu\text{-}MeCO_2)(\mu\text{-edta-}N,N')]^-$ is observed at 362 nm.[32]

The CD spectrum of $[Re_2(\mu\text{-}O)_2\{(R)\text{-pdta}\}_2]^{4-}$ shows a large negative maximum ($\Delta\varepsilon = -24$ M^{-1} cm^{-1}) corresponding to the strong absorption band. This is in sharp contrast with the CD spectrum of the molybdenum(III) dimer $[Mo_2(\mu\text{-}OH)_2(\mu\text{-}MeCO_2)\{\mu\text{-}(R)\text{-pdta-}N,N'\}]^-$, where the CD absorbance in the strong-band region is > 10 times smaller.[37] The latter is consistent with the existence of chirality around the metal ions (ΔΔ) in the rhenium(IV) dimer. Such chirality is absent in the above molybdenum(III) dimer.

Table 5 First-order rate constants (25 °C) for the oxidation of $[Re_2O_2(edta)_2]^{4-}$ (0.05–0.03 mM) with V^V in the presence of V^{IV}, $I = 1.00$ M ($LiClO_4$)

$[H^+]$/M	$10^3[V^{IV}]$/M	$10^3[V^V]$/M	$10^4k_{1obs}/s^{-1}$	$10^4k_{2obs}/s^{-1}$
0.50	4.80	8.00	25.6	19.9
		5.00	18.6	13.3
		4.00	15.1	10.4
		2.67	10.9	6.6
0.30	4.80	8.00	21.7	18.6
		6.00	17.5	14.2
		4.00	12.3	8.9
		2.00	7.70	4.4
		6.00	16.2	11.4
0.17	4.80			
		4.50	11.7	8.5
		3.00	8.75	6.3
		1.50	5.26	2.75
0.10	6.40	4.00	8.17	6.3
		3.33	6.50	5.0
		2.00	4.75	3.1
		1.00	2.58	1.43
	4.80	4.27	9.15	7.3
		3.30	7.48	5.8
		3.00	6.70	4.9
		2.00	4.76	3.4
		1.00	3.02	1.62
	3.20	4.00	11.3	8.9
		3.33	9.79	7.5
		2.00	6.23	4.8
		1.00	4.13	2.38
	1.60	4.00	13.6	10.6
		3.33	11.3	8.8
		2.00	7.62	5.4
		1.00	5.05	2.60
0.075	4.80	2.50	4.54	3.14
		2.00	3.58	2.78
		1.50	2.87	2.00
		1.00	2.31	1.15
0.055	4.80	2.00	2.45	1.70
		1.50	1.90	1.35
		1.00	1.19	0.68
		0.50	1.01	0.36

Oxidation with V^V.—In acidic solution V^V is present as *cis*-$[VO_2(H_2O)_4]^+$, with reduction potential determined as 1.0 V in 1.0 M H^+. The kinetic studies were in the conventional time range ($t_{\frac{1}{2}} \approx 30$ min). For $[H^+]$ in the range 0.05–0.50 M, the dimer is here written as $Re^{IV}{}_2H_2$ although titrations have not demonstrated conclusively whether the fully protonated $[Re^{IV}{}_2(\mu\text{-}O)_2(H_2edta)_2]$ or proton-shared $[Re^{IV}{}_2(\mu\text{-}O)_2(Hedta)_2]^{2-}$ form is present. The stoichiometry of the reaction is 6:1 as in equation (1) with $Re^{IV}{}_2$ oxidised to 2 mol of Re^{VII}. From scan spectra no intermediate oxidation states of Re were detected, but the absorbance decay monitored at 450 nm indicates biphasic kinetics. First-order rate constants k_{1obs} and k_{2obs} are listed in Table 4. Both phases give a first-order dependence on $[V^V]$, Fig. 5. The linear dependencies can be expressed as in equations (2) and (3) with no dependence on $[H^+]$ in the

$$k_{1obs} = a[V^V] + b \quad (2)$$

$$k_{2obs} = c[V^V] \quad (3)$$

Table 6 The variation of rate constants (25 °C) with $[H^+]$ and $[V^{IV}]$, for the first phase (*a* and *b*) and second phase (*c*) of the oxidation of $[Re_2O_2(edta)_2]^{4-}$, I = 1.00 M ($LiClO_4$)

$[H^+]$/M	$10^3[V^{IV}]$/M	a/M^{-1} s^{-1}	10^4b/s^{-1}	c/M^{-1} s^{-1}
0.50	4.80	0.261	4.55	0.252
0.30	4.80	0.236	3.00	0.235
0.17	4.80	0.220	1.75	0.192
0.10	6.40	0.177	0.92	0.156
	4.80	0.190	1.06	0.171
	3.20	0.243	1.58	0.223
	1.60	0.282	2.09	0.265
	0	0.334	2.98	0.316
0.075	4.80	0.148	0.74	0.131
0.055	4.80	0.101	0.50	0.088

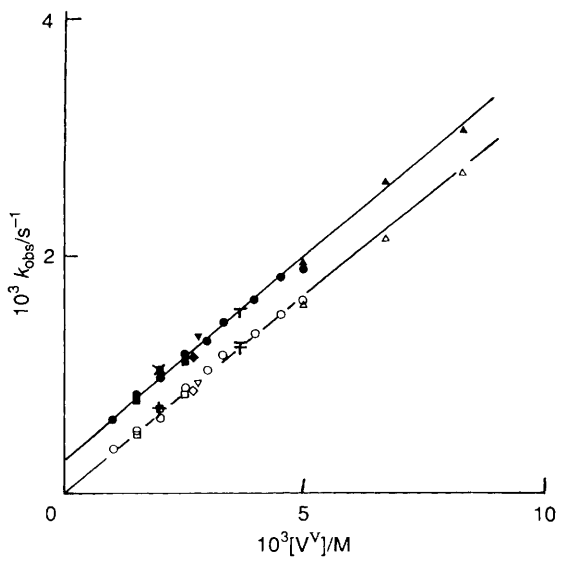

Fig. 5 Dependence on $[V^V]$ of first-order rate constants k_{1obs} (solid) and k_{2obs} (open) at 25 °C for the concurrent (biphasic) oxidation of $[Re_2O_2(edta)_2]^{4-}$ by V^V. No effect is observed on varying $[H^+]$/M = 0.050 (■, □) 0.10 (●, ○) and 0.50 (▲, △) or an addition of Ca^{2+} (◆, ◇), La^{3+} (▼, ▽) and Ti^{IV} (×, +) all 4.8 mM, or with $[Cl^-]$ = 0.15M (T, F). All runs were with I = 1.00M ($LiClO_4$)

range 0.050–0.500 M. At 25 °C, I = 1.00 M ($LiClO_4$), a = 0.331 ± 0.006 M^{-1} s^{-1}, b = (3.18 ± 0.23) × 10^{-4} s^{-1} and c = 0.314 ± 0.005 M^{-1} s^{-1}. The similarity of a and c suggests concurrent reactions involving two isomers of the Re^{IV}_2 complex. An unusual feature is that one of the isomers is able to react with V^V by a V^V-independent path b, which makes possible a distinction between the two forms.

On addition of V^{IV} both k_{1obs} and k_{2obs} (Table 5) decrease, as illustrated in Fig. 6 (in the corresponding plot for k_{2obs} linear plots pass through the origin). The variation of a and c with $[V^{IV}]$ is shown in Fig. 7. Interestingly the rate constants a and c now exhibit an $[H^+]^{-2}$ dependence, *e.g.* Fig. 8 with $[V^{IV}]$ = 4.8 mM. Unlike V^{IV} the cations Ca^{2+}, La^{3+} and Ti^{IV} have no effect on k_{1obs} and k_{2obs}, Table 4 and Fig. 5. The effect of V^{IV} is therefore to suppress the redox process. Table 6 lists values of a, b and c at different $[V^{IV}]$ and $[H^+]$. We consider first the mechanism of a and c. Dependencies on $[H^+]$ can arise from the interplay of the $VO_2^+ + 2H^+ + e^- \longrightarrow VO^{2+} + H_2O$ conversion, protonation of μ-O, or deprotonation of the edta ligands of the Re^{IV}_2 reactant. Some care is required in view of these different possibilities.

A perfectly reasonable redox mechanism incorporating the effects of V^{IV} and $[H^+]$ is as shown in equations (4) and (5). In (5) protonation may be associated with breakdown of the

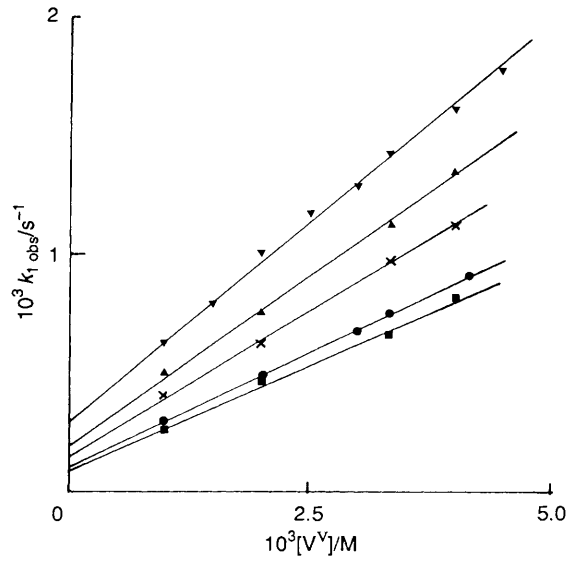

Fig. 6 Effect of $[V^{IV}]$/mM = 6.4 (■), 4.8 (●), 3.2 (×), 1.6 (▲) and 0 (▼) on k_{1obs} (25 °C) for the oxidation of $[Re_2O_2(edta)_2]^{4-}$ by V^V, at $[H^+]$ = 0.10 M, I = 1.00 M ($LiClO_4$)

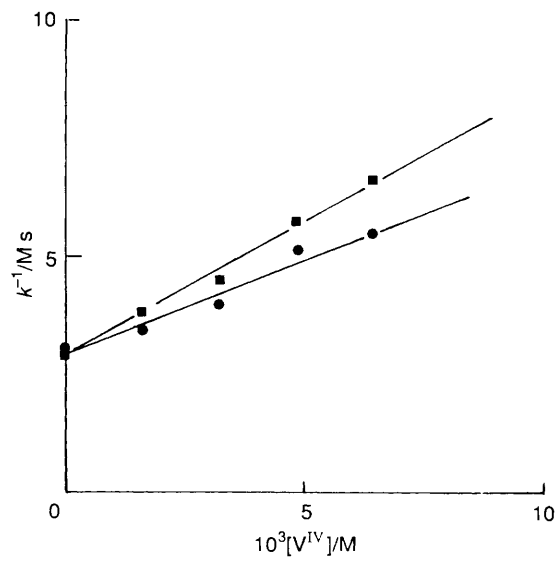

Fig. 7 Dependence on $[V^{IV}]$ of rate parameters a (●) and c (■), here written as k^{-1}, at 25 °C for concurrent reactions in the oxidation of $[Re_2O_2(edta)_2]^{4-}$ by V^V at $[H^+]$ = 0.10 M, I = 1.00M ($LiClO_4$)

$$Re^{IV}{}_2H_2 + V^V \underset{k_2}{\overset{k_1}{\rightleftharpoons}} Re^{IV}Re^V + V^{IV} + 2H^+ \quad (4)$$

$$Re^{IV}Re^V + 2H^+ \xrightarrow{k_3} \text{products} \quad (5)$$

dimer. Applying the stationary-state approximation to the $Re^{IV}Re^V$ intermediate the rate law (6) is obtained, a special case

$$\text{Rate} = \frac{k_1k_3[Re^{IV}{}_2H_2][H^+]^2[V^V]}{k_2[V^{IV}] + k_3[H^+]^2} \quad (6)$$

of which is the experimental rate law $a[Re^{IV}{}_2H_2][V^V]$ in (2) with no V^{IV} present initially. A similar expression holds for c, where the k_1, k_2 and k_3 values can be distinguished by subscripts a and c respectively. Equation (6) will account for the dependencies observed for a and c. Thus using an unweighted least-squares fit, Fig. 9 is a plot of $1/a$ against $[V^{IV}]/[H^+]^2$, from which k_{1a} = 0.286 ± 0.020 M^{-1} s^{-1} and k_{2a}/k_{3a} = 1.09 ± 0.12

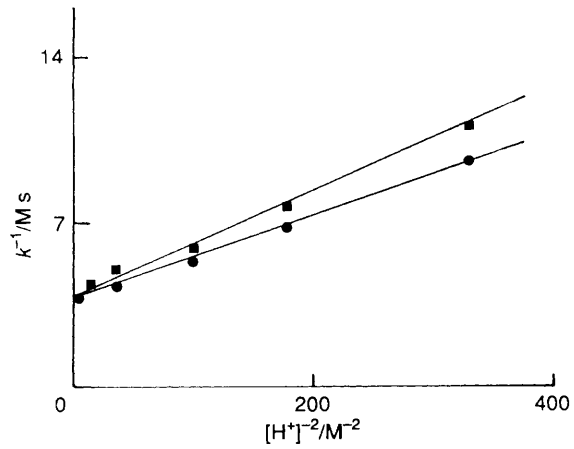

Fig. 8 Dependence on $[H^+]^{-2}$ of rate parameters a (●) and c (■), here written as k^{-1}, at 25 °C for concurrent reactions in the oxidation of $[Re_2O_2(edta)_2]^{4-}$ by V^V at 25 °C, I = 1.00 M ($LiClO_4$)

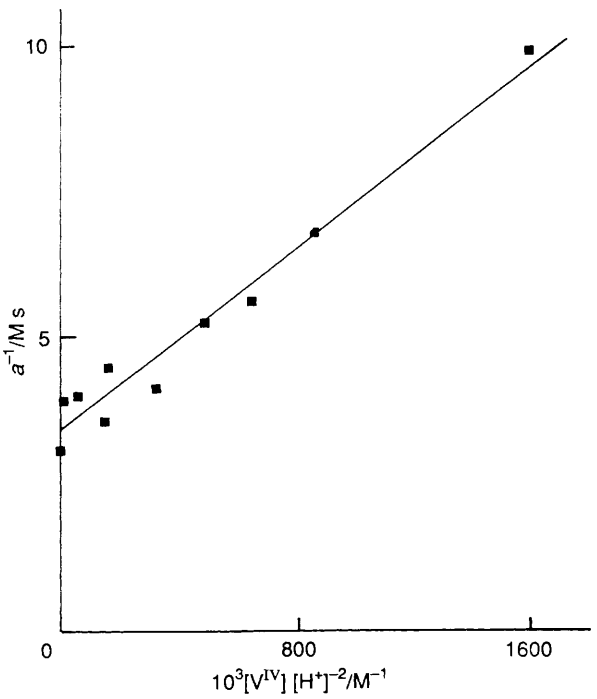

Fig. 9 Dependence of the rate parameter a (25 °C) on $[V^{IV}]/[H^+]^2$ for the oxidation of $[Re_2O_2(edta)_2]^{4-}$ by V^V, I = 1.00 M ($LiClO_4$)

M^{-1} can be evaluated. Owing to the simpler expression (3) for k_{2obs}, the dependence of c can be illustrated, Fig. 10, by plotting $[V^V]/k_{2obs}$ against $[V^{IV}]/[H^+]^2$. From the corresponding fit k_{1c} = 0.292 ± 0.016 M^{-1} s^{-1} and k_{2c}/k_{3c} = 1.64 ± 0.17 M^{-1}. The virtually identical k_{1a} and k_{1c} values and very similar k_2/k_3 ratios are noted.

Owing to proton ambiguities above all else,[38] alternative mechanisms exist. For example an alternative (non-redox) mechanism is indicated in equations (7) and (8). The rate law

$$Re^{IV}{}_2H_2 + V^{IV} \rightleftharpoons Re^{IV}{}_2V^{IV} + 2H^+ \quad (7)$$

$$Re^{IV}{}_2H_2 + V^V \longrightarrow \text{products} \quad (8)$$

obtained by mass balance is of the same form as that in equation (6). In this mechanism V^{IV} displaces $2H^+$ ions in binding to the unco-ordinated carboxylates and by so doing blocks reaction with V^V. The observation that Ca^{2+}, La^{3+} and Ti^{IV} have no similar effect makes this mechanism less likely. However the existence of an inert V=O bond in VO^{2+} it could be argued is

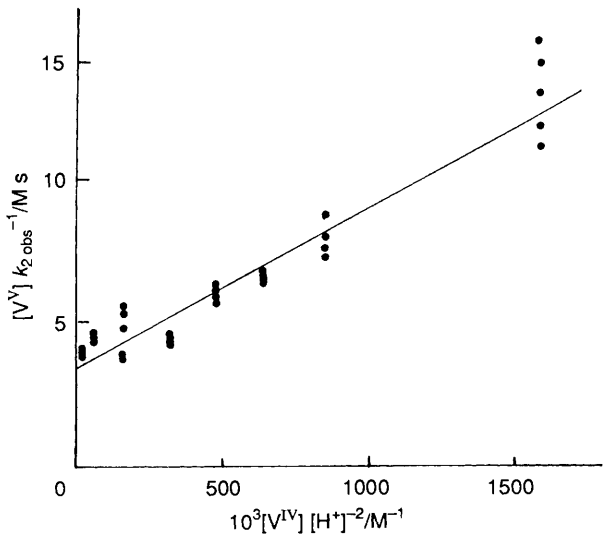

Fig. 10 Linear dependence of $[V^V]/k_{2obs}$ on $[V^{IV}]/[H^+]^2$ for the oxidation of $[Re_2O_2(edta)_2]^{4-}$ by V^V at 25 °C, I = 1.00M ($LiClO_4$)

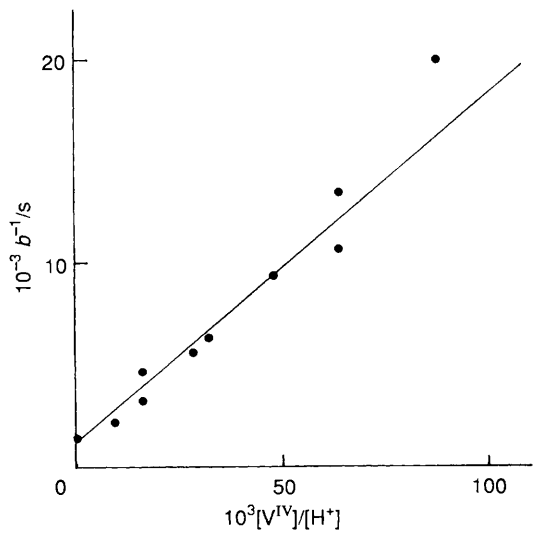

Fig. 11 Variation of b^- with $[V^{IV}]/[H^+]$ for the $[V^V]$-independent pathway in the oxidation of $[Re_2O_2(edta)_2]^{4-}$ by V^V at 25 °C, I = 1.00M ($LiClO_4$)

crucial, whereas in TiO^{2+} the Ti=O bond is known to be much more labile.[39]

The V^V-independent term b implicates the forward reaction (k_4) in equation (9) as a rate controlling step, followed by (10).

$$Re^{IV}{}_2H_2 \xrightarrow{k_4} Re^{IV}{}_2H + H^+ \quad (9)$$

$$Re^{IV}{}_2H + V^V \xrightarrow{\text{fast}} Re^{IV}Re^V + V^{IV} + H^+ \quad (10)$$

The vanadium(IV) inhibition and $[H^+]$ dependence suggest that (11) or a related process is involved. Applying mass balance to equation (11), (12) is obtained. Hence in the presence of V^{IV} the

$$Re^{IV}{}_2H_2 + V^{IV} \overset{K_5}{\rightleftharpoons} Re^{IV}{}_2HV^{IV} + H^+ \quad (11)$$

$$[Re^{IV}{}_2H_2] = \frac{[Re^{IV}{}_2H_2]_T[H^+]}{K_5[V^{IV}] + [H^+]} \quad (12)$$

b term can be expressed as equation (13). A plot of $1/b$ against $[V^{IV}]/[H^+]$ is shown in Fig. 11, from which k_4 = (1.0

$$b = \frac{k_4[H^+]}{K_5[V^{IV}] + [H^+]} \quad (13)$$

$\pm$ 0.8) $\times$ 10^{-3} s^{-1} and K_5 = 191 $\pm$ 18. The large error on k_4 results from the relatively small intercept. The magnitude of k_4 for the acid-dissociation process is comparable to values of $\approx 10^{-5}$ s^{-1} reported for the $H_2O \longrightarrow OH^- + H^+$ dissociation.[40]

To summarise, a particularly interesting kinetic situation arises in the present case with the identification of pathways k_{1obs} and k_{2obs} for two non-interconvertible geometrical isomer forms of the dinuclear Re^{IV}_2 complex $[Re(\mu\text{-}O)_2(edta)_2]^{4-}$. The rate constants *a* and *c* are within 5% of each other and as far as can be ascertained are identical. The distinguishing feature is the V^V-independent term *b*, attributed to a rate-controlling acid-dissociation process (9) followed by (10), which are in competition with (11). This we believe stems from the different distances of pendant carboxylates from each other in the two isomers, and different proton-sharing abilities. The *a* and *b* terms are most likely explained by the redox mechanism in (4) and (5), which is able to account for the inhibition by V^{IV}. However an alternative (non-redox) mechanism involving reaction (7), which might have been expected to proceed with other cations Ca^{2+}, La^{3+} and Ti^{IV}, cannot be entirely ruled out, particularly as it has features in common with (11). No other kinetic stages were observed for the oxidation of $Re^{IV}Re^V$ through to Re^{VII}, and such steps are therefore presumed to be rapid.

Acknowledgements

This work was supported by a Grant-in-Aid for Scientific Research (No. 04214105) on the Priority Area of 'Molecular Approach to Non-equilibrium Processes in Solutions' from the Ministry of Education, Science and Culture, Japan and by the UK SERC (M. N. and B.-L. O.).

References

1 J. Baldas, J. F. Boas, J. Bonnyman, S. F. Colmanet and G. A. Williams, *Inorg. Chim. Acta*, 1991, **179**, 151; J. Baldas, J. F. Boas, Z. Ivanov and B. D. James, *Inorg. Chim. Acta.*, 1993, **204**, 199.
2 (*a*) T. Lis, *Acta Crystallogr., Sect. B*, 1975, **31**, 1594; (*b*) G. Bohm, K. Wieghardt, B. Nuber and J. Weiss, *Inorg. Chem.*, 1991, **30**, 3464.
3 F. A. Cotton and G. Wilkinson, *Advanced Inorganic Chemistry*, 5th edn., Wiley, New York, 1988, p. 831; N. N. Greenwood and A. Earnshaw, *Chemistry of the Elements*, Pergamon, Oxford, 1984, p. 1167.
4 E. I. Stiefel, *Prog. Inorg. Chem.*, 1977, **22**, 1; Z. Dori, *Prog. Inorg. Chem.*, 1981, **28**, 239.
5 G. G. Kneale, A. J. Geddes, Y. Sasaki, T. Shibahara and A. G. Sykes, *J. Chem. Soc., Chem. Commun.*, 1975, 356; G. G. Kneale and A. J. Geddes, *Acta Crystallogr., Sect. B*, 1975, **31**, 1233.
6 A. Bino, F. A. Cotton and Z. Dori, *J. Am. Chem. Soc.*, 1979, **101**, 3842.
7 L. V. Haynes and D. T. Sawyer, *Inorg. Chem.*, 1967, **6**, 2146; B. Spivak and Z. Dori, *J. Chem. Soc., Dalton Trans.*, 1973, 1173; see also A. Kojima, S. Ooi, Y. Sasaki, K. Z. Suzuki, K. Saito and H. Kuroya, *Bull. Chem. Soc. Jpn.*, 1981, **54**, 2457.
8 J. J. Park, M. D. Glick and J. L. Hoard, *J. Am. Chem. Soc.*, 1969, **91**, 301.
9 T. Shibahara, B. Sheldrick and A. G. Sykes, *J. Chem. Soc., Chem. Commun.*, 1976, 523.
10 T. Shibahara, H. Kuroya, K. Matsumoto and S. Ooi, *J. Am. Chem. Soc.*, 1984, **106**, 789.
11 S. Ikari, Y. Sasaki, A. Nagasawa, C. Kabuto and T. Ito, *Inorg. Chem.*, 1989, **28**, 1248.
12 B. Sheldrick, A. B. Soares and A. G. Sykes, *Inorg. Chim. Acta*, 1977, **25**, L83; S. Ikari, Y. Sasaki and T. Ito, *Inorg. Chem.*, 1989, **28**, 447.
13 H.-B. Burgi, G. Anderegg and P. Blauenstein, *Inorg. Chem.*, 1981, **20**, 3829.
14 B. Jezowska-Trzebiatowska and W. Wojciechowski, *Bull. Acad. Pol. Sci.*, 1961, **9**, 685.
15 G. A. Lawrance and D. F. Sangster, *Polyhedron*, 1985, **4**, 1095.
16 F. A. Cotton and B. M. Foxman, *Inorg. Chem.*, 1968, **7**, 1754.
17 L. Wei, T. R. Halbert, R. R. Murray III and E. I. Stiefel, *J. Am. Chem. Soc.*, 1990, **112**, 6431.
18 J. E. Fergusson and J. L. Love, *Aust. J. Chem.*, 1971, **24**, 2689.
19 G. W. Watt and R. J. Thompson, *Inorg. Synth.*, 1963, **7**, 189.
20 F. P. Dwyer and F. L. Garvan, *J. Am. Chem. Soc.*, 1959, **81**, 2955.
21 W. R. Busing and H. A. Levy, *Acta Crystallogr.*, 1957, **10**, 180; J. De Meulenaer and H. Tompa, *Acta Crystallogr.*, 1965, **19**, 1014.
22 *International Tables for X-Ray Crystallography*, Kynoch Press, Birmingham, 1974, vol. 4.
23 T. Sakurai and K. Kobayashi, *Rikagaku Kenkyusho Hokoku*, 1979, **55**, 69.
24 K. E. Linder, J. C. Dewan and A. Davison, *Inorg. Chem.*, 1989, **28**, 3820.
25 G. Anderegg, W. Gasche and K. Zollinger, *Technetium in Chemistry and Nuclear Medicine*, eds. E. Deutsch, M. Nicolini and H. N. Wagner, Verona, 1983, vol. 1, p. 15.
26 F. A. Cotton, R. Eiss and B. M. Foxman, *Inorg. Chem.*, 1969, **8**, 950.
27 C. K. Johnson, ORTEP, Report ORNL-5138, Oak Ridge National Laboratory, Oak Ridge, TN, 1976.
28 K. A. Wilhelmi, E. Lagervall and O. Muller, *Acta Chem. Scand.*, 1970, **24**, 3406.
29 J.-P. Besse, G. Baud, R. Chevalier and M. Gasperin, *Acta Crystallogr., Sect. B*, 1978, **34**, 3532.
30 S. Shaik, R. Hoffman, C. R. Fiesel and R. H. Summerville, *J. Am. Chem. Soc.*, 1980, **102**, 4555.
31 J. Kroubek and J. Podlaha, *J. Inorg. Nucl. Chem.*, 1971, **33**, 2981.
32 T. Shibahara and A. G. Sykes, *J. Chem. Soc., Dalton Trans.*, 1978, 95.
33 E. J. Corey and J. C. Bailar, jun., *J. Am. Chem. Soc.*, 1959, **81**, 2620.
34 G. Anderegg, E. Muller, K. Zollinger and H. B. Burgi, *Helv. Chim. Acta*, 1983, **66**, 1593.
35 K. Wieghardt, M. Hahn, W. Swiridoff and J. Weiss, *Inorg. Chem.*, 1984, **23**, 94.
36 P. Chaudhuri, K. Wieghardt, W. Gebert, I. Jibril and G. Z. Huttner, *Angew. Chem.*, 1985, **521**, 23.
37 Y. Sasaki, T. Tani and S. Morita, *Proceedings of the Climax Fourth International Conference of the Chemistry and Uses of Molybdenum*, eds. H. B. Barry and P. C. H. Mitchell, Climax Molybdenum Company, Ann Arbor, MI, 1982, p. 89.
38 R. D. Cannon, in *Electron Transfer Reactions*, Butterworth, London, 1980, ch. 4, p. 97.
39 P. Comba and A. E. Merbach, *Inorg. Chem.*, 1987, **26**, 1315.
40 See, for example, E. F. Caldin, *Fast Reactions in Solution*, Blackwell Scientific Publications, Oxford, 1964, p. 263.

Received 4*th March* 1993; *Paper* 3/01279D